Ultrabroad emission from a bismuth doped chalcogenide glass

Mark A. Hughes, [1,*]Takao Akada,[1] Takenobu Suzuki,[1] Yasutake Ohishi[1] and Daniel W. Hewak[2]

[1]*Research Center for Advanced Photon Technology, Toyota Technological Institute, 2-12-1 Hisakata, Tempaku, Nagoya 468-8511, Japan*
[2]*Optoelectronics Research Centre, University of Southampton, Southampton SO17 1BJ, United Kingdom*
**mark@toyota-ti.ac.jp*

Abstract: We report emission from a bismuth doped chalcogenide glass which is flattened, has a full width at half maximum (FWHM) of 600 nm, peaks at 1300 nm and covers the entire telecommunications window. At cryogenic temperatures the FWHM reaches 850 nm. The quantum efficiency and lifetime were as high as 32% and 175 μs, respectively. We also report two new bismuth emission bands at 2000 and 2600 nm. Absorption bands at 680, 850, 1020 and 1180 nm were observed. The 1180 nm absorption band was previously unobserved. We suggest that the origin of the emission in Bi:GLS is Bi_2^{2-} dimers.

OCIS codes: (160.3380) General; (300.2530) General science.

References and links

1. M. Peng, D. Chen, J. Qiu, X. Jiang, and C. Zhu, "Bismuth-doped zinc aluminosilicate glasses and glass-ceramics with ultra-broadband infrared luminescence," Opt. Mater. **29**(5), 556–561 (2007).
2. Y. Arai, T. Suzuki, Y. Ohishi, S. Morimoto, and S. Khonthon, "Ultrabroadband near-infrared emission from a colorless bismuth-doped glass," Appl. Phys. Lett. **90**(26), 261110 (2007).
3. M. Peng, B. Wu, N. Da, C. Wang, D. Chen, C. Zhu, and J. Qiu, "Bismuth-activated luminescent materials for broadband optical amplifier in WDM system," J. Non-Cryst. Solids **354**(12-13), 1221–1225 (2008).
4. J. Ren, J. Qiu, B. Wu, and D. Chen, "Ultrabroad infrared luminescence from Bi-doped alkaline earth metal germanate glasses," J. Mater. Res. **22**(6), 1574–1578 (2007).
5. M. Peng, J. Qiu, D. Chen, X. Meng, I. Yang, X. Jiang, and C. Zhu, "Bismuth- and aluminum-codoped germanium oxide glasses for super-broadband optical amplification," Opt. Lett. **29**(17), 1998–2000 (2004).
6. M. Peng, J. Qiu, D. Chen, X. Meng, and C. Zhu, "Superbroadband 1310 nm emission from bismuth and tantalum codoped germanium oxide glasses," Opt. Lett. **30**(18), 2433–2435 (2005).
7. X. G. Meng, J. R. Qiu, M. Y. Peng, D. P. Chen, Q. Z. Zhao, X. W. Jiang, and C. S. Zhu, "Near infrared broadband emission of bismuth-doped aluminophosphate glass," Opt. Express **13**(5), 1628–1634 (2005).
8. X. G. Meng, J. R. Qiu, M. Y. Peng, D. P. Chen, Q. Z. Zhao, X. W. Jiang, and C. S. Zhu, "Infrared broadband emission of bismuth-doped barium-aluminum-borate glasses," Opt. Express **13**(5), 1635–1642 (2005).
9. Y. Fujimoto, and M. Nakatsuka, "Infrared Luminescence from Bismuth-Doped Silica Glass," Jpn. J. Appl. Phys. **40**(Part 2, No. 3B), L279–L281 (2001).
10. X. Wang, and H. Xia, "Infrared superbroadband emission of Bi ion doped germanium-aluminum-sodium glass," Opt. Commun. **268**(1), 75–78 (2006).
11. S. Khonthon, S. Morimoto, Y. Arai, and Y. Ohishi, "Luminescence Characteristics of Te- and Bi-Doped Glasses and Glass-Ceramics," J. Ceram. Soc. Jpn. **115**(1340), 259–263 (2007).
12. V. O. Sokolov, V. G. Plotnichenko, and E. M. Dianov, "Origin of broadband near-infrared luminescence in bismuth-doped glasses," Opt. Lett. **33**(13), 1488–1490 (2008).
13. G. P. Dong, X. D. Xiao, J. J. Ren, J. Ruan, X. F. Liu, J. R. Qiu, C. G. Lin, H. Z. Tao, and X. J. Zhao, "Broadband infrared luminescence from bismuth-doped GeS_2-Ga_2S_3 chalcogenide glasses," Chin. Phys. Lett. **25**(5), 1891–1894 (2008).
14. J. S. Wang, E. M. Vogela, E. Snitzerb, and J. L. Jackela, V. L. Da Silva, and Y. Silberberg, "1.3 μm emission of neodymium and praseodymium in tellurite-based glasses," J. Non-Cryst. Solids **178**, 109–113 (1994).
15. D. W. Hewak, J. A. Medeiros Neto, B. Samson, R. S. Brown, K. P. Jedrzejewski, J. Wang, E. Taylor, R. I. Laming, G. Wylangowski, and D. N. Payne,"Quantum-Efficiency of Praseodymium Doped Ga:La:S Glass for 1.3 mm Optical-Fiber Amplifiers," IEEE Photon. Technol. Lett. **6**(5), 609–612 (1994).
16. I. Abdulhalim, C. N. Pannell, R. S. Deol, D. W. Hewak, G. Wylangowski, and D. N. Payne, "High-performance acousto-optic chalcogenide glass based on Ga_2S_3-La_2S_3 Systems," J. Non-Cryst. Solids **164–166**, 1251–1254 (1993).

#113743 - $15.00 USD Received 2 Jul 2009; revised 1 Sep 2009; accepted 14 Sep 2009; published 12 Oct 2009

17. T. Schweizer, D. W. Hewak, B. N. Samson, and D. N. Payne, "Spectroscopic data of the 1.8-, 2.9-, and 4.3-mm transitions in dysprosium-doped gallium lanthanum sulfide glass," Opt. Lett. **21**(19), 1594–1596 (1996).
18. T. Schweizer, B. N. Samson, and J. R. Hector, W. S. Brocklesby, D. W. Hewak, and D. N. Payne, "Infrared emission from holmium doped gallium lanthanum sulphide glass," Infrared Phys. Technol. **40**(4), 329–335 (1999).
19. M. Hughes, H. Rutt, D. Hewak, and R. Curry, "Spectroscopy of vanadium (III) doped gallium lanthanum sulphide chalcogenide glass. Phys. Lett. **90**(3), 031108 (2007).
20. M. A. Hughes, R. J. Curry, and D. W. Hewak, "Spectroscopy of titanium-doped gallium lanthanum sulfide glass," J. Opt. Soc. Am. B **25**(9), 1458–1465 (2008).
21. M. Peng, C. Wang, D. Chen, J. Qiu, X. Jiang, and C. Zhu, "Investigations on bismuth and aluminum co-doped germanium oxide glasses for ultra-broadband optical amplification," J. Non-Cryst. Solids **351**(30-32), 2388–2393 (2005).
22. C. E. Finlayson, A. Amezcua, P. J. Sazio, P. S. Walker, M. C. Grossel, R. J. Curry, D. C. Smith, and J. J. Baumberg, "Infrared emitting PbSe nanocrystals for telecommunications window applications," J. Mod. Opt. **52**(7), 955–964 (2005).
23. N. C. Greenham, "Measurement of absolute photoluminescence quantum efficiencies in conjugated polymers," Chem. Phys. Lett. **241**(1-2), 89–96 (1995).
24. J. Ren, J. Qiu, D. Chen, X. Hu, X. Jiang, and C. Zhu, "Ultrabroad infrared luminescence from Bi-doped aluminogermanate glasses," Solid State Commun. **141**(10), 559–562 (2007).
25. S. Zhou, H. Dong, H. Zeng, G. Feng, H. Yang, B. Zhu, and J. Qiu, "Broadband optical amplification in Bi-doped germanium silicate glass," Appl. Phys. Lett. **91**(6), 061919 (2007).
26. V. V. Dvoyrin, V. M. Mashinsky, L. I. Bulatov, I. A. Bufetov, A. V. Shubin, M. A. Melkumov, E. F. Kustov, E. M. Dianov, A. A. Umnikov, V. F. Khopin, M. V. Yashkov, and A. N. Guryanov, "Bismuth-doped-glass optical fibers--a new active medium for lasers and amplifiers," Opt. Lett. **31**(20), 2966–2968 (2006).
27. V. V. Dvoyrin, O. I. Medvedkov, V. M. Mashinsky, A. A. Umnikov, A. N. Guryanov, and E. M. Dianov, "Optical amplification in 1430-1495 nm range and laser action in Bi-doped fibers," Opt. Express **16**(21), 16971–16976 (2008).
28. T. Suzuki, and Y. Ohishi, "Ultrabroadband near-infrared emission from Bi-doped Li_2O-Al_2O_3-SiO_2 glass," Appl. Phys. Lett. **88**(19), 191912 (2006).
29. M. Hughes, T. Suzuki, and Y. Ohishi, "Advanced bismuth doped lead-germanate glass for broadband optical gain devices," J. Opt. Soc. Am. B **25**(8), 1380–1386 (2008).
30. J. J. Ren, G. P. Dong, S. Q. Xu, R. Q. Bao, and J. R. Qiu, "Inhomogeneous broadening, luminescence origin and optical amplification in bismuth-doped glass," J. Phys. Chem. A **112**(14), 3036–3039 (2008).
31. A. B. Rulkov, A. A. Ferin, S. V. Popov, J. R. Taylor, I. Razdobreev, L. Bigot, and G. Bouwmans, "Narrow-line, 1178nm CW bismuth-doped fiber laser with 6.4W output for direct frequency doubling," Opt. Express **15**(9), 5473–5476 (2007).
32. M. P. Kalita, S. Yoo, and J. Sahu, "Bismuth doped fiber laser and study of unsaturable loss and pump induced absorption in laser performance," Opt. Express **16**(25), 21032–21038 (2008).
33. E. M. Dianov, S. V. Firstov, V. F. Khopin, A. N. Guryanov, and I. A. Bufetov, "Bi-doped fibre lasers and amplifiers emitting in a spectral region of 1.3 mm," Quantum Electron. **38**(7), 615–617 (2008).
34. Y. Ohishi, "Novel photonics materials for broadband lightwave processing," in *Photonics West*, (SPIE, 2007), 646908.
35. J. A. Duffy, "Redox equilibria in glass," J. Non-Cryst. Solids **196**, 45–50 (1996).
36. J. Ren, J. Qiu, D. Chen, C. Wang, X. Jiang, and C. Zhu, "Infrared luminescence properties of bismuth-doped barium silicate glasses," J. Mater. Res. **22**(7), 1954–1958 (2007).
37. S. Zhou, G. Feng, J. Bao, H. Yang, and J. Qiu, "Broadband near-infrared emission from Bi-doped aluminosilicate glasses," J. Mater. Res. **22**(6), 1435–1438 (2007).
38. M. Y. Peng, C. Zollfrank, and L. Wondraczek, "Origin of broad NIR photoluminescence in bismuthate glass and Bi-doped glasses at room temperature," J. Phys.- Condes. Matter **21**(28), 285106 (2009).
39. B. Denker, B. Galagan, V. Osiko, I. Shulman, S. Sverchkov, and E. Dianov, "Absorption and emission properties of Bi-doped Mg–Al–Si oxide glass system," Appl. Phys. B-Lasers Opt. **95**(4), 801–805 (2009).
40. B. Denker, B. Galagan, V. Osiko, I. Shulman, S. Sverchkov, and E. Dianov, "The IR emitting centers in Bi-doped Mg-Al-Si oxide glasses," Laser Phys. **19**(5), 1105–1111 (2009).
41. V. O. Sokolov, V. G. Plotnichenko, V. V. Koltashev, and E. M. Dianov, "Centres of broadband near-IR luminescence in bismuth-doped glasses," J. Phys. D Appl. Phys. **42**(9), 095410 (2009).
42. T. Ohkura, Y. Fujimoto, M. Nakatsuka, and S. Young-Seok, "Local Structures of Bismuth Ion in Bismuth-Doped Silica Glasses Analyzed Using Bi L_{III} X-Ray Absorption Fine Structure," J. Am. Ceram. Soc. **90**(11), 3596–3600 (2007).
43. K. Moringa, H. Yoshida, and H. Takebe, "Compositional dependence of absorption spectra of Ti^{3+} in silicate, borate, and phosphate glasses," J. Am. Ceram. Soc. **77**(12), 3113–3118 (1994).
44. E. F. Kustov, L. I. Bulatov, V. V. Dvoyrin, and V. M. Mashinsky, "Molecular orbital model of optical centers in bismuth-doped glasses," Opt. Lett. **34**(10), 1549–1551 (2009).

1. Introduction

In recent years bismuth doped glasses have been attracting a lot of attention because many researchers have recognized their potential for broadband amplifiers and tunable lasers. A

#113743 - $15.00 USD Received 2 Jul 2009; revised 1 Sep 2009; accepted 14 Sep 2009; published 12 Oct 2009

wide variety of traditional glass hosts containing Bi have been investigated so far, mainly silicates [1–3] and germanates [4–6] but also phosphates [7] and borates [8]. The product of the emission cross section and lifetime ($\sigma_{em}\tau$), which is inversely proportional to the laser threshold, has often been calculated and is usually found to be considerably higher than traditional laser materials such as Ti:sapphire. However, arguably the most interesting property of Bi doped glasses is the very large width of emission, which sets them apart from traditional rare earth dopants such as erbium and neodymium. In some hosts, the emission can cover the technologically useful low loss window of silica ~1300-1700 nm, otherwise known as the telecommunications window. This leads to the possibility of developing a broadband optical amplifier covering all possible telecommunication wavelengths. This could replace or complement the erbium doped fiber amplifier (EDFA), which is currently used in fibre optic networks but is limited by its relatively narrow gain bandwidth. The origin of the infrared emission from Bi doped glasses remains controversial and has been attributed to Bi^{+} [8], Bi^{5+} [9, 10], Bi metal clusters [6] and negative charged Bi_2 dimers [11, 12].

Although there are numerous reports of Bi emission from traditional glasses we are only aware of one report of emission from a chalcogenide (GeS_2-Ga_2S_3) [13]. Chalcogenide glasses often exhibit low phonon energy, this allows the observation of certain transitions in rare earth dopants that are not observed in traditional glasses such as silica. For example, it is virtually impossible to measure 1.3 μm fluorescence from the $^1G_4 \rightarrow {}^3H_5$ transition of Pr^{3+} in silica-based glass, but it has been observed in tellurite glass [14] and its efficiency approaches 60% in a chalcogenide glass [15]. With respect to the observation of unusual emission transitions a particularly notable glass is gallium lanthanum sulphide (GLS). GLS has a transmission window of ~0.5-10 μm [16], a high refractive index of ~2.4 which results in high radiative emission rates, and a low maximum phonon energy of ~425 cm^{-1} which results in low non-radiative decay rates [17]. These effects have led to high quantum efficiencies for transitions with a small energy gap to the next lower lying energy level [15]. GLS has also allowed the observation of low energy transitions which are not seen in other hosts. For example, the first observation of the 4.9 μm fluorescence from the $^5I_4 \rightarrow {}^5I_5$ transition of Ho^{3+} was in a GLS host [18]. Unusual emission from V^{3+} has also been observed in GLS [19], as well as rarely observed Ti^{3+} emission in a glass host [20]. In this work we report the absorption, excitation, emission (from excitation wavelengths of 480-1300 nm), quantum efficiency (QE), lifetime and cryogenic spectral measurements of Bi doped GLS

2. Experimental

2.1 Glass melting

A sample of Bi:GLS was prepared by mixing 70% gallium sulphide, 23% lanthanum sulphide, 6% lanthanum oxide and 1% bismuth sulphide (% molar). Batching was carried out in a dry-nitrogen purged glove box. Melt components were batched into a vitreous carbon crucible and weighed using a balance with a resolution of 0.001g. The batch was then transferred to a furnace using a custom built closed atmosphere transfer pod. Gallium and lanthanum sulphides were synthesised in-house from gallium metal (9N purity) and lanthanum fluoride (5N purity) precursors in a flowing H_2S gas system. Before sulphurisation lanthanum fluoride was purified and dehydrated in a dry-argon purged furnace at 1250 °C for 36 hours to reduce OH^- and transition metal impurities. The lanthanum oxide and bismuth sulphide were purchased commercially and used without further purification. The glass was melted at 1150°C for around 24 hours, in a silica tube furnace, with an initial ramp rate of 20 °C min^{-1} and under a constant argon atmosphere (flow of 200 ml min^{-1}). This method was chosen in favor of the sealed ampoule method because volatile impurities such as OH^- are carried downstream away from the melt and because of safety concerns about the ampoules exploding. The melt was rapidly quenched to form a glass by pushing the crucible holder into a silica water jacket. The quenching process is designed to prevent crystallization of the glass by rapidly increasing the viscosity of the glass through a rapid temperature drop, hence arresting the nucleation and growth of crystals. The glass was then annealed at 400 °C for 12

#113743 - $15.00 USD Received 2 Jul 2009; revised 1 Sep 2009; accepted 14 Sep 2009; published 12 Oct 2009

hours. The resulting glass contained a dark marbling pattern indicating that the Bi was not distributed evenly in the sample or had partly been incorporated as the black suboxide BiO [21]. However, all optical measurements were carried out on a transparent section of the sample with a size of 1mm x 5mm x 5mm. This may mean that the transparent section had a lower Bi content than the rest of the sample. However, emission spectra taken on the rest of the sample were very similar to the transparent section. Since this sample was the first trial melt we believe we can improve the transparency and homogeneity by reducing the Bi content, mixing the raw materials before melting, modifying the melt temperature, time and atmosphere.

2.2 Spectroscopic measurements

Absorption spectra were taken on a Perkin Elmer Lambda 900 spectrophotometer over a range of 175-3300nm with a resolution of ±0.1nm. Various laser sources were used to obtain emission spectra: assorted laser diodes at wavelengths between 650 and 1215 nm, a Ti:sapphire laser at wavelengths between 700 and 1000 nm and a Lotis Tii LT-2215 optical parametric oscillator (OPO) pumped by Q-switched UV laser at wavelengths between 480 and 1300 nm. The laser diodes were electronically modulated, giving a 1/e fall time of ~250 ns, whereas the Ti:sapphire laser beam was focused with a microscope objective and modulated with a mechanical chopper at the focus waist, which gave a 1/e fall time of ~20 μs. Emission spectra were obtained by dispersing the fluorescence generated by laser sources in a Jasco CT-25C monochromator, using gratings blazed at 1000 or 2000 nm, the slit width was ~1 mm which corresponded to a resolution of ~4 nm. Various filters were used to block the excitation light. Detection was realized with a Hamamatsu H9170 NIR photomultiplier tube (PMT), which was sensitive from 950 to 1650 nm and had a fall time of 1.7 ns; a Hamamatsu G5852-11 InGaAs detector, which was sensitive from 750 to 2200 nm and had a fall time of 27 μs; and a Teledyne Judson J15D12 mercury cadmium telluride (MCT) detector, which was sensitive from 1.5 to 12 μm and had a fall time of 1 μs. This was coupled with standard phase sensitive detection. All spectral measurements were corrected for the wavelength dependent response of the measurement system by calculating a correction spectra ($C(\lambda)$) with: $C(\lambda)=I_{cal}(\lambda)/I_{meas}(\lambda)$. Where $I_{meas}(\lambda)$ is the luminescence spectrum of an Ushio calibrated white light source measured by the detection system and $I_{cal}(\lambda)$ is the luminescence spectrum of the calibrated white light source supplied by the manufacturer. In various instances filters were unable to block the excitation light. In these cases we took advantage of the high switching speed of the laser diodes and the fast response time of the PMT by taking a spectrum at a low modulation frequency of ~100 Hz ($I_{low}(\lambda)$); this spectrum contained both emission and excitation signals. We then took a spectrum at a very high modulation frequency of ~70 KHz $I_{high}(\lambda)$, at this frequency the emission was rejected because of its decay time but the excitation was not. We then obtained a spectrum of the emission only ($I_{em}(\lambda)$) by subtracting them: $I_{em}(\lambda)=I_{low}(\lambda)-I_{high}(\lambda)$. Transient fluorescence measurements were made with the PMT detector and a Yokogawa DL1620 200MHz oscilloscope and averaged ~10000 times.

QE measurements were taken with the same system used for emission measurements except that the sample was placed in a Labsphere 4P-GPS-040-SF integrating sphere with a diameter of ~10 cm, and the signal was detected with the Hamamatsu G5852-11 InGaAs detector. The samples were mounted behind a baffle such that there was no direct line-of-sight between the sample and the exit port, and angled such that reflected excitation light was directed away from the entrance port. For QE measurements with 650 nm excitation we used a fiber coupled integrating sphere. The output from this integrating sphere was coupled into a large core bundled fibre which could be changed between two different spectrometers, used to detect the excitation and emission, with a high repeatability. The emission was detected with a Photal MCPD-5000 multi channel photo detector and the excitation was detected with a Hamamamatsu C7473 multichannel analyzer, these spectrometers were calibrated against each other using the white light source. A “photons out / photons in” method, similar to that described in refs [22, 23] for calculating the quantum efficiency was used. The number of photons absorbed was taken to be proportional to the difference between the area under the

#113743 - $15.00 USD Received 2 Jul 2009; revised 1 Sep 2009; accepted 14 Sep 2009; published 12 Oct 2009

laser line spectrum with the sample present ($I_{sample}(\lambda)$) and without the sample present ($I_{sphere}(\lambda)$). The number of photons emitted was taken to be proportional to the area under the emission spectrum ($I_{PL}(\lambda)$). The spectra were corrected with a correction spectra ($C(\lambda)$). A correction for photon energy was also made, since a higher photon flux is required at longer wavelengths to produce the same irradiance per unit area than at shorter wavelengths, by multiplying by the wavelength. Hence the quantum efficiency (η_{QE}) was calculated with Eq. (1):

$$\eta_{QE} = \frac{\int \lambda I_{PL}(\lambda) C(\lambda) d\lambda}{\int \lambda I_{sphere}(\lambda) C(\lambda) d\lambda - \int \lambda I_{sample}(\lambda) C(\lambda) d\lambda} \quad (1)$$

QE measurements were taken three times to give an average and estimate of error. Cryogenic measurements were taken by placing the sample in a closed cycle He gas cryostat.

3. Results and discussion

3.1 Room temperature spectral measurements

Figure 1 shows the absorption spectra of Bi doped GLS and un-doped GLS. The un-doped absorption spectrum is typical of GLS, showing a strong electronic absorption edge at ~550 nm. In the Bi:GLS absorption spectrum a shoulder can be identified at around 850 nm, there is also a redshift of the bandedge which indicates there is a Bi absorption band at ~600 nm. The Bi:GLS sample shows a background absorption caused by the low transparency of the sample.

Figure 2 shows a contour plot which represents the emission spectra taken at various excitation wavelengths. The excitation source was the OPO which was varied between 480 and 1300 nm in increments of 10 or 20 nm. We measured the excitation power at each excitation wavelength and used this to normalize the emission spectra for the varying excitation power. The emission intensity is shown in a log scale so that the weak emission bands can be seen along side the stronger ones. Two strong emission bands can be seen with excitation peaks at 680 and 850 nm, these relate to the absorption bands identified in Fig. 1. Two weaker emission bands can be seen with excitation peaks at 1020 and 1180 nm. These excitation peaks identify 4 absorption bands at 680, 850, 1020 and 1180 nm. This compares to absorption bands at ~500, 700, 800 and 1000 nm which are commonly observed in various Bi doped silicates and germanates [24, 25]. A weak Bi absorption band at 1400 nm has also been identified in Bi doped silica glass [26, 27]. The absorption band at 1020 nm also appears much narrower than previous reports. Furthermore, to the best of our knowledge, this is the first time an absorption band at 1180 nm has been identified in a Bi doped glass.

#113743 - $15.00 USD Received 2 Jul 2009; revised 1 Sep 2009; accepted 14 Sep 2009; published 12 Oct 2009

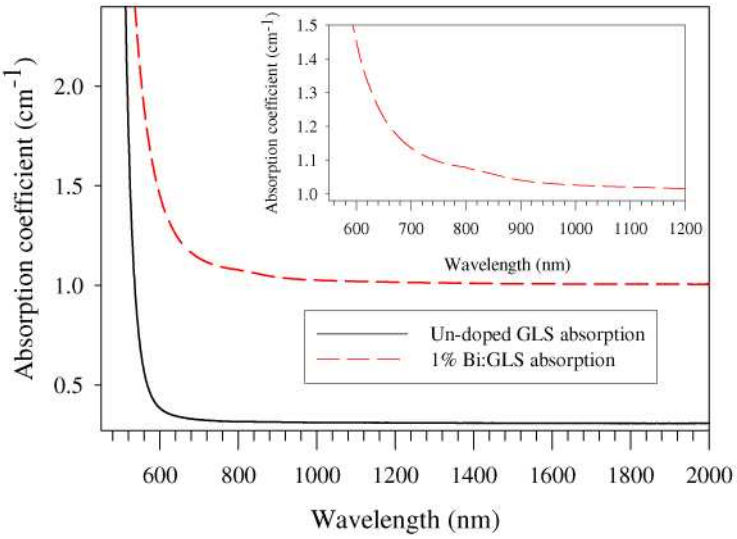

Fig. 1. Absorption spectra of 1% Bi doped GLS and un-doped GLS. The inset shows a close-up of the Bi:GLS absorption

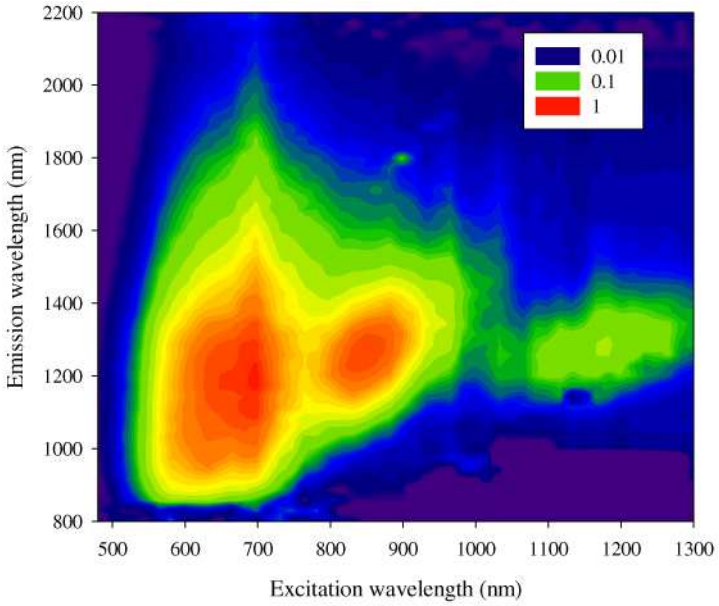

Fig. 2. Contour plot showing the emission spectra, normalized to the excitation power, of Bi doped GLS at excitation wavelengths of 480-1300 nm. Emission intensity is in a log scale.

Figure 3 shows the full width at half maximum (FWHM) as a function of excitation wavelength of the emission spectra shown in Fig. 2, these were taken with the OPO. There is a strong dependence of FWHM on excitation wavelength. The most striking feature is the peak in FWHM at 1020 nm excitation. This coincides with the narrow 1020 nm absorption band identified in Fig. 2. Figure 3 also shows the QE at various excitation wavelengths. The QE reaches a maximum of 32% with 900 nm excitation. Comparing the dependence of QE and FWHM indicates a trade-off between QE and FWHM.

#113743 - $15.00 USD Received 2 Jul 2009; revised 1 Sep 2009; accepted 14 Sep 2009; published 12 Oct 2009

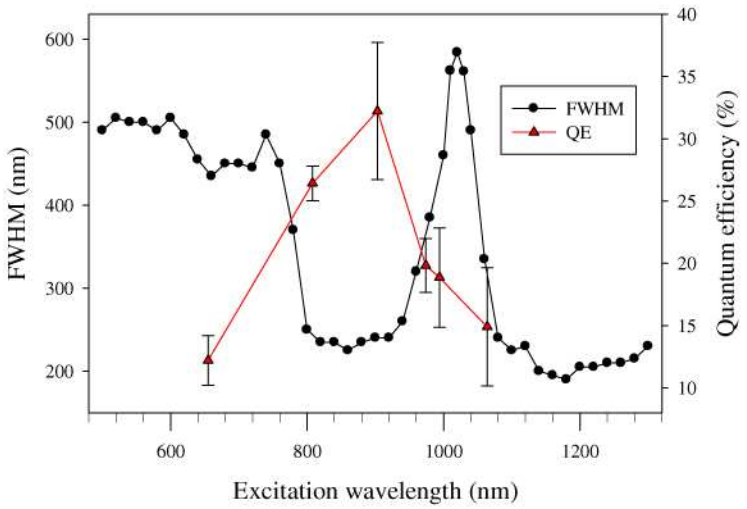

Fig. 3. Emission FWHM and quantum efficiency as a function of excitation wavelength.

Examples of the some emission spectra, from excitation wavelengths of 755, 974, 1020 and 1064 nm, are shown in Fig. 4. Excitation at 755 nm produces a single emission band peaking at 1220 nm with a FWHM of 482 nm. This is similar to the emission from lithium-alumino-silicate glass excited at 800 nm [28]. 1064 nm excitation produces a peak in a similar position, except it is narrower, and there is a second emission band at 1580 nm. A similar emission band was observed in Bi doped strontium-alumino-germanate glass [4]. When the excitation is 974 nm the peak shifts to 1350 nm. This is somewhat unusual since 974 nm excitation usually produces emission peaking at ~1100 nm in Bi doped glasses [4, 28–30]. The emission from 1020 nm excitation is exceptional since it results in the largest FWHM of 600 nm and it covers the entire telecommunications window, the spectra is also flattened over the O, E and S bands. The width of this emission equals the current broadest reported emission from a Bi doped glass which was from a Bi doped soda-lime-silicate glass excited at 720 nm [2]. However, the emission in ref [2] consisted of two rather separated peaks at 870 and 1200 nm and it did not cover any of the telecommunications window. The fact that this broad emission results from 1020 nm excitation is also important because previous reports of lasing in Bi doped glasses tend to come from long excitation wavelengths. For example, the excitation wavelengths of various Bi doped glass lasers are: 1070 nm [31], 1080 nm [32] and 1205 nm [33]. The QE at 1020 nm excitation is ~17% which compares favorably to the 11% QE reported for Bi doped alumino-silicate glass [34].

#113743 - $15.00 USD Received 2 Jul 2009; revised 1 Sep 2009; accepted 14 Sep 2009; published 12 Oct 2009

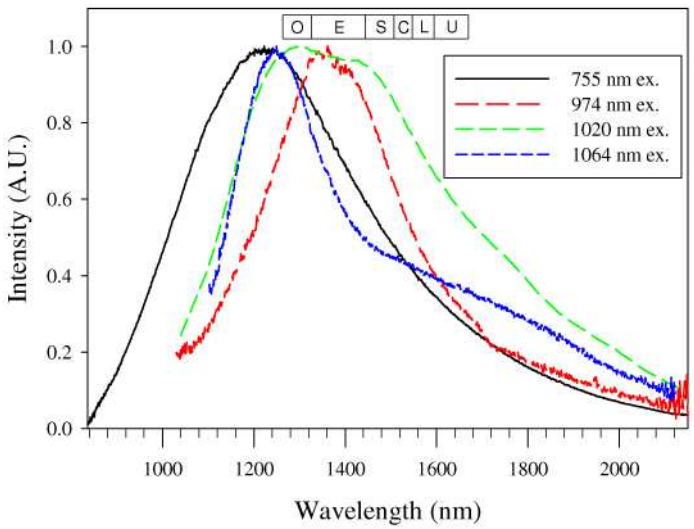

Fig. 4. Examples of emission spectra at excitation wavelength 755, 974, 1020 and 1064 nm. The standard telecommunication bands are also shown.

3.2 Cryogenic spectral measurements

We measured the emission from Bi:GLS at cryogenic temperatures with 808, 974 and 1020 nm excitation. The emission narrowed slightly at excitation wavelengths of 808 and 1020 nm, however, at 974 nm excitation the emission became much broader. At low temperatures we could detect stray excitation light in the emission spectrum, to correct for this we used the method described in section 2.2. Three detectors were used in these emission spectra: the PMT over 1000-1650 nm, the InGaAs over 1000-2200 nm and the MCT over 1900-2800 nm; there were good overlaps between the emission spectra from the different detectors which indicates that the system correction was valid.

Figure 5 (a) shows the emission spectra from 974 nm excitation at temperatures of 5-300 K. As the temperature decreases new emission bands at ~1200 and 1500 nm appear to be formed, as well as longer wavelength emission bands. Figure 5 (b) shows the deconvolution of the emission spectrum at 5 K into Gaussians. The number of Gaussians was determined by the minimum number required to give a coefficient of determination (R^2) > 0.995. The deconvolution suggests four Gaussian bands (1, 2, 3 and 4) centered at 1200, 1500, 2000 and 2600 nm, respectively. To the best of our knowledge, this work is the first time that emission bands from Bi at 2000 and 2600 nm have been reported. We believe that the reason we are able to observe these low energy emission bands is a combination of the cryogenic temperatures and the unusually low phonon energy of GLS. In higher phonon energy glasses and at higher temperatures they may decay non-radiatively by coupling to phonon modes.

#113743 - $15.00 USD Received 2 Jul 2009; revised 1 Sep 2009; accepted 14 Sep 2009; published 12 Oct 2009

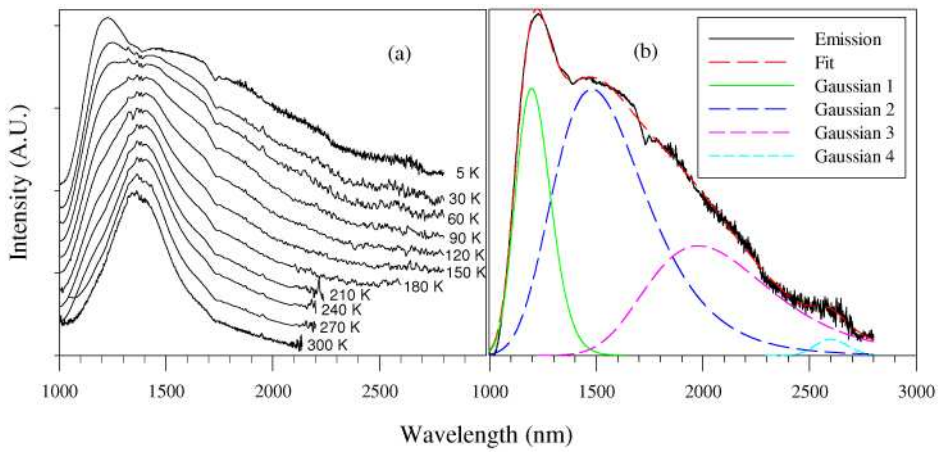

Fig. 5. Emission spectra from 974 nm excitation at temperatures 5-300 K (a), deconvolution of the emission spectra at 5 K into Gaussians (b).

The FWHM of the emission as a function of temperature for 808 and 974 nm excitation is shown in Fig. 6. For 808 nm excitation a small shoulder at ~1450 nm appeared in the emission spectrum at cryogenic temperatures. The emission FWHM decreased slightly from 300 nm at 300 K to 280 nm at 5 K, as would be expected from a depopulation of higher order phonon modes. However, the small relative decrease in FWHM indicates that the main broadening mechanism is inhomogeneous, such as a range of crystal field strengths. For 974 nm excitation the FWHM increases monotonically with decreasing temperature. This is caused by the appearance of new emission bands. The FWHM reaches 850 nm at 5 K. This is by far the broadest emission from a Bi doped glass at any temperature, and to the best of our knowledge the broadest emission from any active ion in this wavelength region.

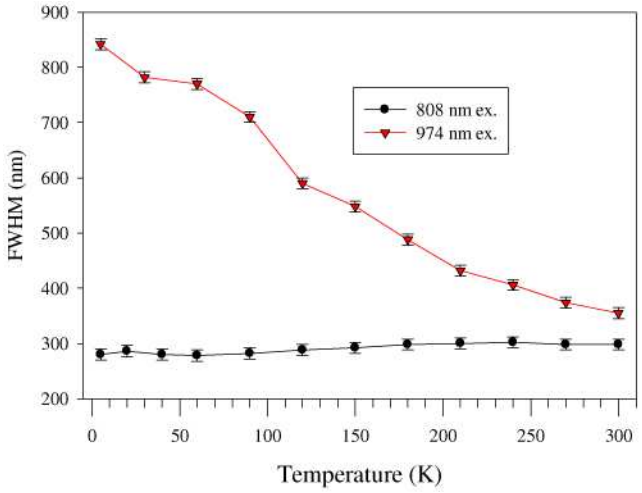

Fig. 6. Emission FWHM as a function of temperature for excitation wavelengths of 808 and 974 nm.

3.3 Lifetime measurements

Figure 7(b) shows an example of the emission decay from 808 nm excitation, measured at a wavelength of 1450 nm. This decay, along with all the other emission decays we measured, was highly non-exponential. As a result, we calculated the lifetime using the average lifetime function [24] $\tau = \int tI(t)dt / \int I(t)dt$.

#113743 - $15.00 USD Received 2 Jul 2009; revised 1 Sep 2009; accepted 14 Sep 2009; published 12 Oct 2009

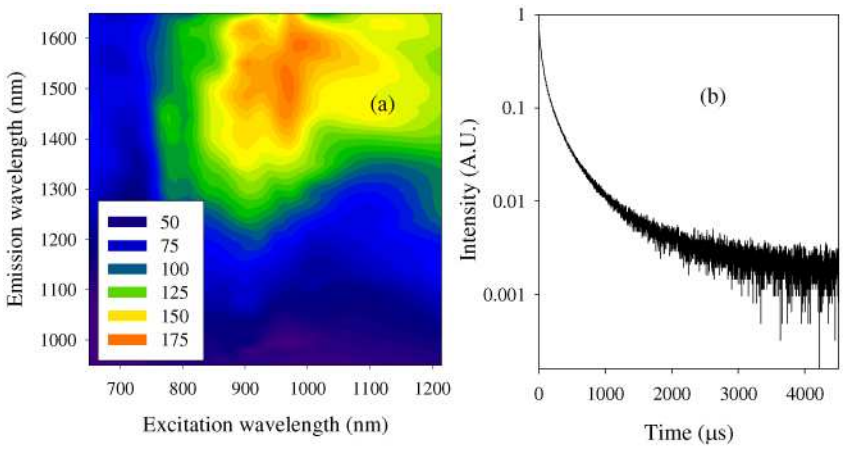

Fig. 7. Room temperature lifetime (μs) as a function of excitation and emission wavelength (a). Example of an emission decay (b).

Figure 7 (a) shows the lifetime as a function of emission and excitation wavelength. It shows there is a peak in lifetime of ~175 μs at emission and excitation wavelengths of ~1500 and 980 nm, respectively. This peak in lifetime corresponds approximately with the ultrabroad emission from 1020 nm excitation, where the lifetime drops to ~160 μs. This is important when considering Bi:GLS as a gain medium for a broadband amplifier or laser because it means the technologically extremely useful emission from 1020 nm excitation has close to the maximum lifetime of Bi:GLS.

3.4 Origin of emission

As mentioned previously, there is much controversy over the origin of IR emission in Bi doped glasses. Bi^{2+} and Bi^{3+} can be excluded as origins of Bi emission in glasses because in crystals these ions have very different emission properties from those of Bi doped glasses [7]. Bi^{+} has been suggested as the origin of emission in Bi doped glasses based on the optical basicity theory proposed by Duffy [35], which states that a higher basicity of glass favors higher valence states of multivalent metal ions. Ren *et al* found that Bi emission decreased with increases in BaO content and with the radius of either BaO, SrO or CaO glass components [36]. This indicated that the concentration of Bi emission centers decreased with increasing basicity of the glass. Zhou *et al* reported that the addition of basic oxides (Na_2O and K_2O), which would favor high valence Bi, reduced the intensity of Bi emission [37]. Also, Bi absorption and emission disappears with the addition of the oxidizing agent, CeO_2, to Bi doped alumino-silicate glass. This would favor the formation of high valence Bi [37]. However, the addition of reducing agents such as carbon increased the Bi emission intensity in Bi doped soda-lime-silicate glass [2]. Also Pb^0, which is isoelectric with Bi^{+}, shows similar emission wavelengths, absorption wavelengths, bandwidths and lifetimes [37]. Bi^0 has been suggested as the origin of emission based on comparisons of atomic spectral data [38].

Bi_2 dimers and BiO have been suggested as the origin of the emission since in a gas phase they have emission characteristics similar to Bi doped glasses [1]. A quadratic dependence of absorption strength on Bi concentration has also been suggested as evidence for Bi_2 dimers [39, 40]. Other evidence for Bi_2 dimers includes electron spin resonance (ESR) measurements of Bi doped silicate glass and glass-ceramics which showed similarities to ESR spectra of other dimer molecules [11] and modeling of energy levels [12, 41]. The observation in this work of Bi emission in Bi:GLS, which has a very low oxygen content, and in a non-oxygen containing chalcogenide glass [13] detracts from BiO being the origin of emission.

Bi^{5+} is another suggested origin of Bi emission since there was no ESR signal of unpaired Bi electrons in Bi doped silica glass. This indicated the presence of Bi^{3+} or Bi^{5+} [9]. X-ray

#113743 - $15.00 USD Received 2 Jul 2009; revised 1 Sep 2009; accepted 14 Sep 2009; published 12 Oct 2009

absorption fine structure (XAFS) measurements showed that the Bi-O distance in Bi doped silica glass was similar to that of Bi^{5+} in crystals [42].

The arguments in favor of the various origins of Bi emission are often contradictory. However, in our opinion arguments for Bi^{+} and Bi_2 are stronger than those for Bi^{5+} since they relate more directly to observed emission and absorption properties. The deoxidized argon atmosphere that we used in melting Bi:GLS is reducing. The same atmosphere has been shown to favor lower valence states of Ti in Ti doped silicate glass [43]. This discredits Bi^{5+} being the origin of emission.

We examined various published energy level models of Bi doped glasses to see if our emission bands at 2000 and 2600 could be accounted for. These models included a molecular orbital model of a BiO_4 molecule [44] and a model based on quantum-chemical calculations of Bi_2^- and Bi_2^{2-} dimers [12, 41]. By examining the low-lying states of a Bi_2^{2-} dimer (Fig. 2, ref [12].) we found that the emission transitions $^1\Sigma_0 \rightarrow {}^3\Sigma_0^+$ and $^1\Sigma_0^- \rightarrow {}^3\Sigma_0^+$ appeared to have wavelengths of 1920 and 2330 nm, respectively. This is in reasonable agreement with the emission bands that we observed and it is the only model of Bi emission in glasses that we are aware of that can account for the 2000 and 2600 nm emission bands in Bi:GLS. We therefore suggest that the origin of the emission in Bi:GLS is Bi_2^{2-} dimers.

4. Conclusions

In this paper we report for the first time, to the best of our knowledge, emission form a Bi doped glass with a FWHM of 600 nm which is flattened and covers the telecommunications window. The excitation wavelength, QE and lifetime of this emission was 1020 nm, 17% and 160 μs, respectively. The maximum QE was 32% at 900 nm excitation. At cryogenic temperatures the FWHM reached 850 nm with 974 nm excitation and we observed two new bismuth emission bands at 2000 and 2600 nm. Emission measurements taken with excitation wavelengths of 480-1300 nm revealed 4 absorption bands at 680, 850, 1020 and 1180 nm. The 1180 nm absorption band was previously unobserved. The maximum room temperature lifetime of 175 μs occurred at emission and excitation wavelengths of ~1500 and 980 nm, respectively. By examining previously published models of Bi emission in glasses to see if they could account for the 2000 and 2600 nm emission bands we suggest that the origin of the emission in Bi:GLS is Bi_2^{2-} dimers.

Acknowledgments

This work was supported by MEXT, the Private University High-Tech Research Center program (2006-2010).

#113743 - $15.00 USD Received 2 Jul 2009; revised 1 Sep 2009; accepted 14 Sep 2009; published 12 Oct 2009